ELSEVIER

Int. J. Electron. Commun. (AEÜ) **58** (2004): 93–99
http://www.elsevier-deutschland.de/aeue

International Journal AEÜ of **Electronics** and **Communications**

Efficient Scattering Calculations in Complex Backgrounds

Olivier J. F. Martin

Dedicated to Professor Reinhold Pregla on the occasion of his 65th birthday

Abstract: The utilization of the Green's tensor associated with a complex optical background (surface, cavity or stratified medium) leads to a dramatic reduction of the computation effort associated with scattering calculations in that background. This approach is illustrated with examples where a mere change of the background Green's tensor makes possible the investigation of completely different physical situations. Two different discretization approaches are compared and similarities between the Green's tensor technique and the Method of Lines are emphasized; in the latter, the utilization of analytic solutions in one specific direction also reduces the discretization of the system.

Keywords: Electromagnetics, Scattering, Modeling, Numerical techniques, Method of lines, Green's tensor

1. Introduction

The complexity of modern photonic components is such that the simulation of light scattering and propagation in these systems is becoming extremely challenging [1]. To overcome these difficulties, one can pursue two different approaches: either one uses a brute force approximate method such as the beam propagation technique or finite differences time domain, to handle the complete system and obtain usually an approximate description; or one develops a computational tool which includes a great deal of insights into the physics of the system, thereby reducing the numerical effort so that the problem becomes tractable while the solution remains accurate. Remark that for smaller problems – that could also in principle be handled accurately with a brute force technique – the second approach provides a much more efficient framework for the simulation of the system, giving usually more accurate results with a smaller computational effort.

From a discretization point of view, a brute force approach leads to the discretization of the entire system, as illustrated in Fig. 1(a). This discretization can be dramatically reduced by a computational approach based on the mathematical structure associated with the system, in particular with the background in which the scatterers are embedded. In this article, we shall describe two such approaches, the Method of Lines (MoL) and the Green's tensor technique, which discretizations are illustrated in Fig. 1(b) and (c).

Received September 1, 2003. Revised January 15, 2004.

Nanophotonics and Metrology Laboratory, School of Engineering STI-NAM, Swiss Federal Institute of Technology Lausanne EPFL, 1015 Lausanne, Switzerland. Fax: +41-21-693.26.14.
E-mail: oliver.martin@epfl.ch

The MoL was originally developed to solve partial differential equations [2, 3] and was first applied to the study of planar metallic and dielectric microwave structures in the early 1980's [4–6]. Over the past twenty years, the MoL has been extensively developed by R. Pregla and collaborators [7, 8]. The versatility of the technique is such that it can be applied to numerous physical configurations relevant to modern optical and microwave technology, such as complex microwave structures [9–14], photonic components [15–18]. The MoL can also handle periodic structures [19–21] and stratified backgrounds [22–24]. Further, subtle effects at the interface between optics and microwave, like for example in traveling wave photodetectors, can also be investigated with the MoL [24].

Since the vectorial character of the fields is included in the calculation, anisotropic media where some of these components are coupled can also be investigated [25, 26]. The MoL can be used both for the propagation/scattering of electromagnetic fields and for the computation of eigenmodes. Recently, it was utilized for the calculation of the dispersion relations of surface plasmons propagating at optical frequencies on subwavelength metallic waveguides, an extremely important and difficult problem of nanophotonics [27, 28].

The discretization principle of the MoL is illustrated in Fig. 1(b) for the case of scattering by a defect embedded in a stratified background. While a standard brute force approach requires the discretization of the entire system, the MoL only requires a discretization in one direction, e.g. x-direction in Fig. 1(b), while analytical solutions are used along the other direction, e.g. along the dashed lines in Fig. 1(b). The computational effort is hence reduced by one dimension. Further, the utilization of analytical functions to solve the problem in one specific direction strongly increases the accuracy of the solution, compared to alternative, more expensive, fully numerical approaches. The boundary conditions are also treated more accurately with the MoL. This is particularly important for mode calculations, where inaccurate boundary conditions can influence the eigenstates of the system under study.

It should be emphasized that the MoL stems from the astute utilization of the symmetry of the background in which the scatterers are embedded. In this article, we would like to present another approach, which also uses the mathematical structure associated with that background to reduce the computational effort and increase the accuracy of the solution. This approach is based on the electric field integral equation and utilizes the dyadic Green's tensor. The key here is that the Green's tensor associated with certain types of backgrounds, such as a sur-

1434-8411/04/58/02-093 $ 30.00/0

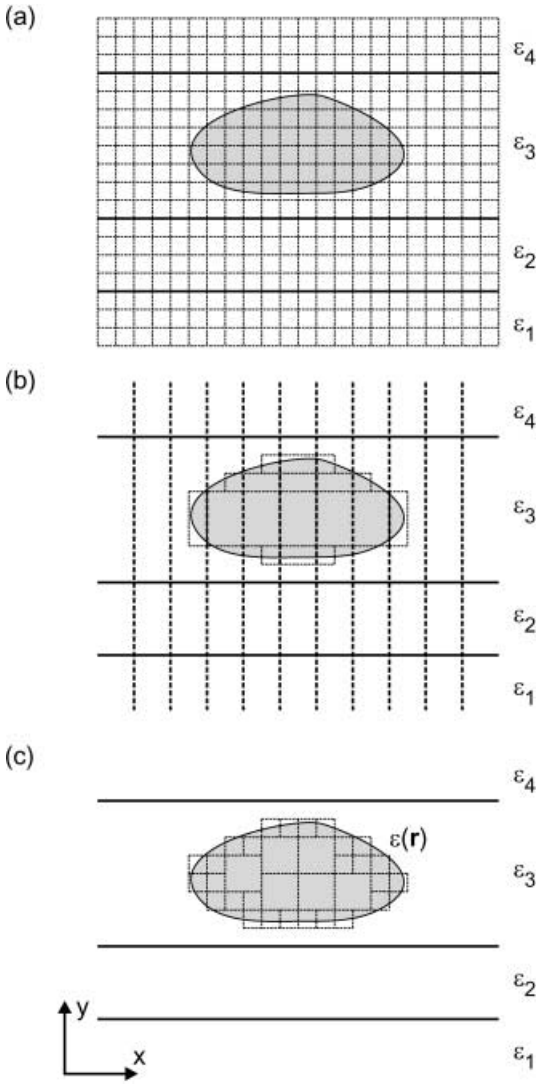

Fig. 1. Different approaches to the discretization of a system composed of a scatterer embedded a stratified background with four layers of different permittivities. (a) Brute force approach, where the entire system is discretized. (b) Method of lines approach, where analytic solutions are used in one direction, e.g. along the dashed lines, and the discretization occurs only along the other direction, leading to a piecewise homogeneous structure in the vertical direction. (c) In the Green's tensor approach, the background is accounted for analytically and the entire scatterer must be discretized in both directions.

face, a stratified medium or a cavity, can be a-priori calculated. Once this is done, the discretization required for the calculation of the system composed of scatterers embedded in the background can be limited to the scatterers. This is illustrated in Fig. 1(c) with a similar example to that previously handled with the MoL. Once the Green's tensor associated with the background is known (either numerically or analytically), the scattering calculation can proceed by merely discretizing the scatterers, the background being accounted for in the Green's tensor.

The objective of this article is twofold. First I would like to compare and evidence some similarities between two different discretization approaches for the Green's tensor technique, which were developed over the last few years [29, 30]. In particular, I will show that one technique can be obtained as a special case of the other. Second, the key role played by the background in scattering phenomena will be emphasized by investigating the same object placed in different backgrounds.

The article is organized as follows: The formalism of the Green's tensor technique is developed in Sect. 2, where the general equations are derived. Numerical implementation using either finite differences or finite elements is discussed in Sect. 3. The influence of the dielectric background on scattering calculations is illustrated in Sect. 4, a summary is given in Sect. 5.

2. Formalism

The Green's tensor technique can be developed in a very general manner by considering one or several scatterers described by a dielectric function $\varepsilon(\mathbf{r})$ and embedded in a background. The latter can take different forms: e.g. an infinite homogeneous background with permittivity ε_{B} [29]; a surface or a stratified medium, composed of several material layers with different permittivities [31–33] $\varepsilon_{\mathrm{Bi}}$, as illustrated in Fig. 1(c); or a cavity with metallic walls [34].

When this system is illuminated with an incident field $\mathbf{E}^0(\mathbf{r})$ propagating in the background, the total electric field $\mathbf{E}(\mathbf{r})$ (incident field plus scattered field) is a solution of the vectorial wave equation

$$\nabla \times \nabla \times \mathbf{E}(\mathbf{r}) - k_0^2\, \varepsilon(\mathbf{r})\, \mathbf{E}(\mathbf{r}) = 0\,, \qquad (1)$$

where $k_0^2 = \omega^2/c^2$ is the vacuum wave number (throughout the paper we assume non-magnetic materials and an $\exp(-i\omega t)$ time dependence for the fields).

Although the present formalism can easily handle anisotropic scatterers described by a tensorial dielectric function, for the sake of simplicity we limit the discussion to scalar dielectric functions. A tensorial dielectric $\varepsilon(\mathbf{r})$ is simply accounted for by replacing the product $\varepsilon(\mathbf{r})\,\mathbf{E}(\mathbf{r})$ with the corresponding contraction $\varepsilon(\mathbf{r}) \cdot \mathbf{E}(\mathbf{r})$.

Introducing the dielectric contrast

$$\Delta\varepsilon(\mathbf{r}) = \varepsilon(\mathbf{r}) - \varepsilon_{\mathrm{B}}\,, \qquad (2)$$

we can rewrite Eq. (1) as an inhomogeneous equation

$$\nabla \times \nabla \times \mathbf{E}(\mathbf{r}) - k_0^2\, \varepsilon_{\mathrm{B}}\, \mathbf{E}(\mathbf{r}) = k_0^2\, \Delta\varepsilon(\mathbf{r})\, \mathbf{E}(\mathbf{r})\,, \qquad (3)$$

where the incident field $\mathbf{E}^0(\mathbf{r})$ must be a solution of the corresponding homogeneous equation:

$$\nabla \times \nabla \times \mathbf{E}^0(\mathbf{r}) - k_0^2\, \varepsilon_{\mathrm{B}}\, \mathbf{E}^0(\mathbf{r}) = 0\,. \qquad (4)$$

To compute the total field $\mathbf{E}(\mathbf{r})$, let us introduce the Green's tensor $\mathbf{G}(\mathbf{r}, \mathbf{r}')$ associated with the background ε_{B}. This dyadic is a solution of the vector wave

equation (4) with a point source term [35]:

$$\nabla \times \nabla \times \mathbf{G}(\mathbf{r}, \mathbf{r}') - k_0^2 \varepsilon_\mathrm{B} \mathbf{G}(\mathbf{r}, \mathbf{r}') = \mathbf{1}\delta(\mathbf{r} - \mathbf{r}') , \qquad (5)$$

where $\mathbf{1}$ is the unit dyad.

Introducing Eq. (5) into Eq. (3), it is a simple matter to find that the total field $\mathbf{E}(\mathbf{r})$ is given by

$$\mathbf{E}(\mathbf{r}) = \mathbf{E}^0(\mathbf{r}) + \int_\mathrm{V} \mathrm{d}\mathbf{r}' \mathbf{G}(\mathbf{r}, \mathbf{r}') \cdot k_0^2 \Delta\varepsilon(\mathbf{r}') \mathbf{E}(\mathbf{r}') , \qquad (6)$$

where the integration runs over the entire volume V of the different scatterers in the system.

The scatterers need not being homogeneous, but $\varepsilon(\mathbf{r})$ can vary inside each scatterer. Finally, the permittivity of the scatterers must not necessarily be higher than their surrounding and, e.g., holes in a dielectric layer can be accounted for using a negative dielectric contrast $\Delta\varepsilon(\mathbf{r})$ [36]. This can also be used to study scattering in microcavities [29].

The incident field $\mathbf{E}^0(\mathbf{r})$ in Eq. (1) must be a solution of the wave equation in the background. Depending on the latter, different types of fields can be used, giving to the Green's tensor technique quite some flexibility, as will be illustrated in Section 4.

Since by definition $\Delta\varepsilon(\mathbf{r}) = 0$ in the background outside these scatterers, the integration in Eq. (6) runs only on the volume of the different scatterers $\varepsilon(\mathbf{r})$ in the structure. This is the key of the Green's tensor technique, it allows limiting the discretization of Eq. (6) to the scatterers, the background being accounted for by the Green's tensor. Equation (6) also indicates that the scattered field at any point of the background is entirely determined by the field inside the scatterer. This can be used to split the calculation: in a first step only the field inside the scatterer is computed and stored; the field at any desired location in the background being then computed at a later stage.

A word of caution should be given here with respect to the singular behavior of the Green's tensor in Eq. (6) when $\mathbf{r} \to \mathbf{r}'$ [37]. Mathematically speaking, one must take the principal value of Eq. (6), as explained in detail in Ref. [29]. From a practical point of view, this singularity can be handled using a small exclusion volume when a finite differences discretization of Eq. (6) is used; for a finite elements discretization, generalized functions can be utilized to extract the singularity by removing that associated with the scalar Green's function and integrating the latter over the basis function [30]. When the observation point $\mathbf{r}$ is located outside the scatterer, no singularity shows up since the integration in Eq. (6) is limited to the scatterer volume.

3. Discretized equations

The scatterer (or scatterers if there is more than one) can be arbitrarily positioned within the background. In the case of a stratified background, they can for example extend over several layers. In the case of such stratified background made of different materials, the dielectric contrast in Eq. (2) is defined with respect to the material layer at the location of the scatterer.

To obtain a system of ordinary equations to be solved for the unknown scattered field $\mathbf{E}(\mathbf{r})$, two different approaches can be used. In general, a simple finite differences scheme can be directly applied to Eq. (6), as will be discussed first [29]. Recently, we also developed a finite elements solution to this problem, which will be presented in the following section [30]. It is important to notice that the discretization scheme is completely independent of the background type, which renders this technique extremely versatile.

3.1 Finite differences

To solve Eq. (6) numerically, let us define a grid with N meshes over the system. Each mesh i is centered at position $\mathbf{r}_i$ and has a volume V_i, $i = 1, \ldots, N$ (for 2D systems V_i represents the area of the mesh). A regular mesh with constant volume V_i is not mandatory and a higher mesh refinement can be used where a precise knowledge of the field is required or where the dielectric contrast $\Delta\varepsilon(\mathbf{r})$ is large, as illustrated in Fig. 1(b).

Introducing the discretized field $\mathbf{E}_i = \mathbf{E}(\mathbf{r}_i)$, the discretized dielectric contrast $\Delta\varepsilon_i = \Delta\varepsilon(\mathbf{r}_i)$ and the discretized Green's tensor $\mathbf{G}_{i,j} = \mathbf{G}(\mathbf{r}_i, \mathbf{r}_j)$, we can rewrite Eq. (6) as a dense system of linear equations:

$$\mathbf{E}_i = \mathbf{E}_i^0 + \sum_{j=1}^{N} \mathbf{G}_{i,j} \cdot k_0^2 \Delta\varepsilon_j \mathbf{E}_j \mathrm{V}_j \qquad (7)$$

for $i = 1, \ldots, N$. Formally, Eq. (7) does not hold for $j = i$, as $\mathbf{G}_{i,j}$ diverges in that case. As mentioned, a simple regularization scheme based on the Cauchy principal value of Eq. (6) must be used to handle this singularity, as described in [29, 37].

3.2 Finite elements

There are three main limitations in the finite differences discretization of Eq. (6): first, the electric field is approximated with peace-wise constant functions and cannot be known in an arbitrary point; second, cubic shape meshes used to discretized the geometry are often inappropriate to describe non-regular surfaces; third, the singularity of the Green's tensor is handled in an approximate manner, with an accuracy that does not improve when the size of the mesh decreases. This impinges on the convergence of the technique, as the singularity of the Green's tensor leads to exploding fields when the mesh size decreases.

To overcome these limitations, we recently introduced an alternative approach to discretize Eq. (6), based on finite elements [30]. In that case, we divide the scatterers into N tetrahedra (triangles in 2D) with volumes $\mathcal{V}_\alpha$ (surfaces $\mathcal{V}_\alpha$ in 2D), $\alpha = 1, \ldots, N$. On each element α we assume a constant dielectric contrast $\Delta\varepsilon_\alpha$ and define m scalar basis functions $f_\alpha^1, \ldots, f_\alpha^m$ that vanish outside α.

For the field $\mathbf{E}(\mathbf{r})$ inside the scatterer we write

$$\mathbf{E}(\mathbf{r}) = \sum_{\alpha=1}^{N} \sum_{j=1}^{m} \mathbf{a}_\alpha^j \, f_\alpha^j, \tag{8}$$

with $\mathbf{a}_\alpha^j$ the unknown vectorial coefficients. Inserting Eq. (8) in Eq. (6), symmetrizing by multiplication with $\Delta\varepsilon(\mathbf{r})$ and applying Galerkin's scheme [38], we obtain the system of $mN \times mN$ vectorial equations

$$\sum_{j=1}^{m} b_\alpha^{ij} \mathbf{a}_\alpha^j - \sum_{\beta=1}^{N} \sum_{j=1}^{m} \mathbf{d}_{\alpha\beta}^{ij} \cdot \mathbf{a}_\beta^j = \mathbf{e}_\alpha^i, \;\; \begin{matrix} i = 1, \ldots, m \\ \alpha = 1, \ldots, N \end{matrix} \tag{9}$$

with

$$b_\alpha^{ij} = \Delta\varepsilon_\alpha \int_{\mathcal{V}_\alpha} \mathrm{d}\mathbf{r} \, f_\alpha^i(\mathbf{r}) \, f_\alpha^j(\mathbf{r}), \tag{10}$$

$$\mathbf{e}_\alpha^i = \Delta\varepsilon_\alpha \int_{\mathcal{V}_\alpha} \mathrm{d}\mathbf{r} \, f_\alpha^i(\mathbf{r}) \mathbf{E}^0(\mathbf{r}), \tag{11}$$

$$\mathbf{d}_{\alpha\beta}^{ij} = \Delta\varepsilon_\alpha V_\beta \int_{\mathcal{V}_\alpha} \mathrm{d}\mathbf{r} \, f_\alpha^i(\mathbf{r}) \int_{\mathcal{V}_\beta} \mathrm{d}\mathbf{r}' \mathbf{G}(\mathbf{r}, \mathbf{r}') \, f_\beta^j(\mathbf{r}'). \tag{12}$$

The numerical solution of Eq. (9) gives the unknown coefficients for the field inside the scatterer. The field outside the scatterer can then be determined from the field inside the scatterer using Eq. (6).

Standard Gaussian integration technique is applied to evaluate the integrals in Eqs. (10)–(12). To carry out this numerical quadrature, each finite element α is mapped onto a canonical element with a linear transformation. Like this, Gaussian points and weights defined on the canonical elements can be used [39, 40].

To handle the divergence of the Green's tensor with finite elements, a special regularization scheme must be introduced. The main idea here is to subtract from the integrand a function with the same singular behavior, but which can be integrated analytically on a triangle (2D) or a tetrahedron (3D), as explained in detail in [30].

While the finite differences gives a peace-wise constant representation of the electric field within the scatterer, the finite elements allows the calculation of the field at any location in the scatterers using the continuous basis functions. Further, since tetrahedric meshes are used with the finite element scheme, arbitrary shape scatterers can be better approximated.

The finite differences scheme presented in Sect. 3.1 can be obtained as a special case of the finite elements discretization described in this section, by using constant basis functions and Dirac delta functions as test functions. In that case, Eqs. (9)–(12) lead exactly to a symmetrize version of Eq. (7). However, this requires another type of finite elements as the Galerkin scheme, with different sets of basis and test functions [38].

3.3 Green's tensor

The Green's tensor represents the response of a point source in the background medium. More precisely, each column β of the 3×3 matrix $G_{\alpha\beta}(\mathbf{r}, \mathbf{r}')$ gives the 3 components $\alpha = x, y, z$ of the electric field radiated at position $\mathbf{r}$ by a dipole located at position $\mathbf{r}'$ and oriented in the β-direction ($\beta = x, y, z$).

For an infinite homogeneous background, this dyadic is just the field radiated directly from $\mathbf{r}'$ to $\mathbf{r}$ and has a simple analytical form [29]. This is not the case for a surface, a stratified background, or a cavity. In that case, the field radiated at $\mathbf{r}$ by a dipole located at $\mathbf{r}'$ must also include the field reflected and refracted at any interface in the background. No analytical expressions exist in this case and the Green's tensor must usually be computed numerically [31–34]. This is quite a complicated task, that is best accomplished by expressing the Green's tensor in the reciprocal space of the background (Fourier space) and using the symmetry properties of the background in that space. The Green's tensor is then obtained in direct space via inverse Fourier transform, i.e. via a numerical quadrature (so-called Sommerfeld integral). This quadrature, which represents the core of the computation is intricate as it involves several poles and branch cuts associated with the different electromagnetic modes that can be excited in the background. However, once the Green's tensor associated with the background is known, the entire discretization can be restricted to the embedded scatterers.

Note that the Green's tensor associated with the background has some additional intrinsic physical properties, which can be useful for investigating active sources such as fluorescent molecules or quantum dots embedded in the background [41–43].

3.4 Solution of the discretized equations

The system of equation resulting from the discretization [Eqs. (7) or (9)] is best solved numerically using an iterative solver [44, 45]. Let us mention that for specific backgrounds, the Green's tensor does not have the same symmetry properties as in an infinite homogeneous space. In particular:

$$\mathbf{G}(\mathbf{r}, \mathbf{r}') \neq \mathbf{G}(\mathbf{r} - \mathbf{r}') \, . \tag{13}$$

It is therefore not possible to rewrite Eqs. (6) as a convolution and use a 3D fast Fourier transform to perform the integration [46]. It is however possible to use reduced symmetry properties in one specific plane to expedite the computation [47].

It should be noted that when the dielectric contrast is strong or the scatterers volume important, the condition number of the matrix associated with Eqs. (7) or (9) becomes quite large, thereby requiring an extremely stable matrix solver. Iterative solvers such as conjugate gradients seem particularly well suited for that task [44].

4. Illustration of the influence of the background

The utilization of the Green's tensor technique for complex scattering calculations is illustrated in this section. By using a scatterer of similar shape placed in different backgrounds, we emphasize the influence of the background and of the illumination mode on the behavior of the system.

The geometry of the first example is shown in Fig. 2(a): we consider the scattering by a dielectric cube made of glass (permittivity $\varepsilon = 2.25$, side $a = 1\,\mu\text{m}$) illuminated with a plane wave incident on its lower left corner at 45°, TM-polarized with a vacuum incident wavelength $\lambda = 1\,\mu\text{m}$. The scatterer is embedded in an infinite homogeneous background with permittivity ε_B. Figure 2(b), respectively 2(c), give the total electric field intensity when the background is air ($\varepsilon_\text{B} = 1$), respectively water ($\varepsilon_\text{B} = 1, 8$).

When the contrast between the scatterer and the background is high, strong scattering occurs, leading to an important standing wave in front of the cube [Fig. 2(b)]. A modal structure develops inside the cube, as its dimensions are larger than the effective wavelength in the dielectric. A focusing effect is also visible at the top right corner of the scatterer. This effect appears even stronger in the case of a water background, Fig. 2(c). In that case, the backscattering is weaker, leading to smaller field values and a grayish figure [the same gray scale is used for Fig. 2(b) and (c)]. Notice also the smaller period for the standing wave in front of the cube for the water background, as the illumination wavelength is accordingly reduced. Although the background here is extremely simple, the ability to handle water opens many important applications, especially in biosensing, where optical diagnostics are now routinely used and optical simulations can help interpret the corresponding data.

Very different results are obtained if the cube is now placed in a stratified background, as illustrated in Fig. 3(b). The background is composed of five layers and defines two high permittivity slab waveguides with a 200 nm thickness, separated with an air gap of 1.9 μm. The embedded scatterer has now a side $a = 1.5\,\mu\text{m}$ and is made of the same high permittivity material [Fig. 3(a)]. As illumination field we now choose the TM mode of the bottom waveguide at $\lambda = 1.5\,\mu\text{m}$.

The corresponding field intensity distribution is shown in Fig. 3(b). A strong mode is excited in the cavity, which couples to the waveguide in spite of the large separation distance between them. Some energy is even transferred to the upper waveguide. Since this coupling is purely resonant, the field distribution in the upper guide is mainly dictated by the cavity mode and the energy transport in the forward direction in that guide remains negligible.

Since the Green's tensor is a fully vectorial approach, subtle effects, such as polarization coupling and crosstalks could also be investigated in that context [29, 48]. However, in the case of the single high symmetry resonator presented here, they remain very weak.

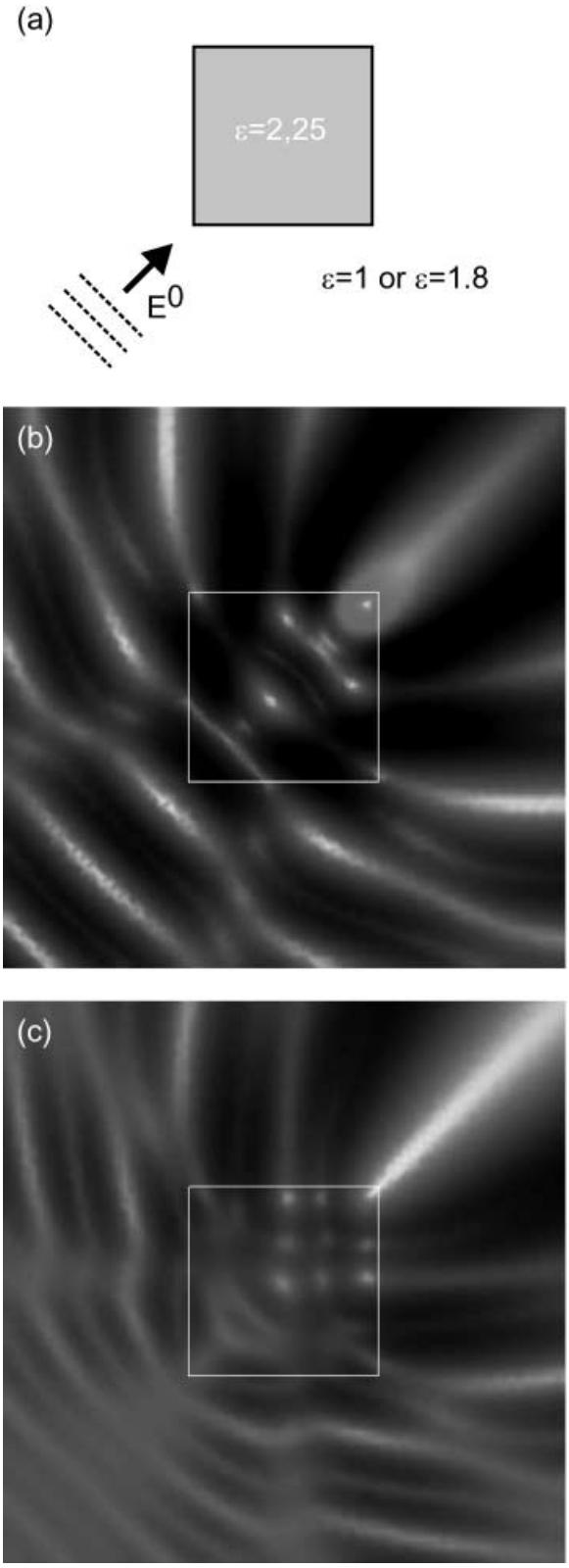

Fig. 2. Scattering by a cube in an infinite homogeneous background: (a) geometry and illumination field, (b) field intensity distribution for a vacuum background ($\varepsilon_\text{B} = 1$), (c) field intensity distribution for a water background ($\varepsilon_\text{B} = 1.8$).

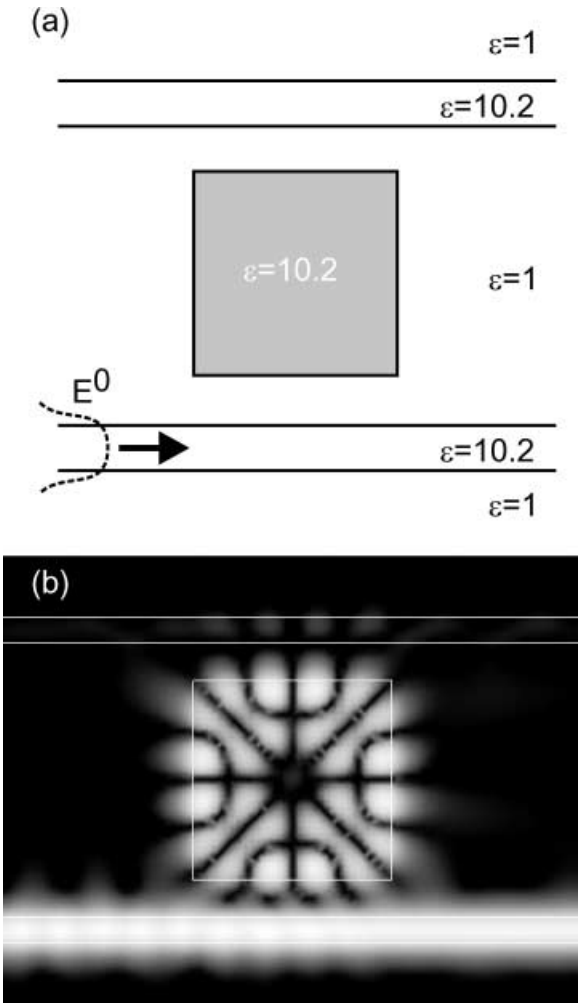

Fig. 3. Scattering by a cube located between two high index waveguides: (a) geometry (b) field intensity distribution under illumination through the bottom waveguide.

5. Summary

The Green's tensor technique is advantageous since only a limited part of the system must be discretized, the background been accounted for by the Green's tensor. The price to pay for this is a-priori knowledge of the Green's tensor, which computation can be time consuming for certain backgrounds. The possibility to split the calculation into two steps (first the calculation of the field inside the scatterer and then the calculation of the field at any required point in the background) is also advantageous. It allows a minimal calculation in the first step, while the field in the background can be calculated later from the field in the scatterers. One drawback of the approach is the fact that it leads to full matrices, which require a fair amount of data storage for their solution.

Finally, as for the MoL which has been widely used in microwave as well as in optics, it should be mentioned that the Green's tensor technique is also used for microwaves, especially in the context of antennae design [49–51].

Acknowledgement. I am delighted to have this opportunity to acknowledge many stimulating discussions with R. Pregla over the years during which I was developing the formalism of the Green's tensor technique.

References

[1] Baets, R.; Dhoedt, B.; Heremans, P.; Paineau, S.; Mennerat, S.: Technologies for optical interconnects between CMOS ics. Proc. SPIE, 1998. 546–549.
[2] Liskovets, O. A.: The method of lines. Differential'nye Uravneniya **1** (1965), 1662–1678.
[3] Michlin, S. G.; Smolizki, C.: Näherungsmethoden zur Lösung von Differential- und Integralgleichungen. Leipzig: Teubner, 1969, 238–243.
[4] Schulz, U.; Pregla, R.: A new technique for the analysis of the dispersion characteristics of planar waveguides [microstrip line analysis]. Archiv für Elektronik und Übertragungstechnik **34** (1980), 169–173.
[5] Worm, S. B.; Pregla, R.: Hybrid mode analysis of arbitrarily shaped planar microwave structures by the method of lines. IEEE Transactions on Microwave Theory and Techniques **32** (1984), 191–196.
[6] Diestel, H.: A method for calculating the guided modes of strip-loaded optical waveguides with arbitrary index profile. IEEE J. Quantum Electron. **20** (1984), 1288–1293.
[7] Pregla, R.; Pascher, W.: Numerical techniques for microwave and millimeter wave passive structures. New York: J. Wiley, 1989, Ch. The method of lines, 381–446.
[8] Pregla, R.; Pascher, W.: Recent res. develop. in microwave theory and techniques. Singpost, 2002, Ch. Modeling of microwave devices with the method of lines, 145–196.
[9] Pascher, W.; Pregla, R.: Full wave analysis of complex planar microwave structures. Radio Science **22** (1987), 999–1002.
[10] Pascher, W.; Pregla, R.: Analysis of rectangular waveguide junctions by the method of lines. IEEE Transactions on Microwave Theory and Techniques **43** (1995), 2649–2653.
[11] Vietzorreck, L.; Pregla, R.: Hybrid analysis of three-dimensional MMIC elements by the method of lines. IEEE Transactions on Microwave Theory and Techniques **44** (1996), 2580–2586.
[12] Vietzorreck, L.; Pascher, W.: Modeling of conductor loss in coplanar circuit elements by the method of lines. IEEE Transactions on Microwave Theory and Techniques **45** (1997), 2474–2478.
[13] Pregla, R.: The analysis of general axially symmetric antennas with a coaxial feed line by the method of lines. IEEE Transactions on Antennas and Propagation **46** (1998), 1433–1443.
[14] Pregla, R.: Efficient and accurate modeling of planar anisotropic microwave structures by the method of lines. IEEE Transactions on Microwave Theory and Techniques **50** (2002), 1469–1479.
[15] Pregla, R.; Ahlers, E.: Method of lines for analysis of discontinuities in optical waveguides. Electronics Letters **29** (1993), 1845–1847.
[16] Rogge, U.; Pregla, R.: Method of lines for the analysis of dielectric waveguides. Journal of Lightwave Technology **11** (1993), 2015–2020.

[17] Pregla, R.: The method of lines for the analysis of dielectric waveguide bends. Journal of Lightwave Technology **14** (1996), 634–639.
[18] Conradi, O.; Helfert, S.; Pregla, R.: Comprehensive modeling of vertical-cavity laser-diodes by the method of lines. IEEE Journal of Quantum Electronics **37** (2001), 928–935.
[19] Ctyroky, J; Helfert, J.; Pregla, R.: Analysis of a deep waveguide Bragg grating. Opt. Quantum Elec. **30** (1998), 343–358.
[20] Goncharenko, I.; Helfert, S.; Pregla, R.: General analysis of fibre grating structures. Journal of Optics A: Pure and Applied Optics **1** (1999), 25–31.
[21] Pregla, R.: Efficient modeling of periodic structures. AEU International Journal of Electronics and Communications **57** (2003), 185–189.
[22] Pregla, R.; Yang, W.: Method of lines for analysis of multilayered dielectric waveguides with bragg gratings. Electronics Letters **29** (1993), 1962–1963.
[23] Kremer, D.; Pregla, R.: The method of lines for the hybrid analysis of multilayered cylindrical resonator structures. IEEE Transactions on Microwave Theory and Techniques **45** (1997), 2152–2155.
[24] Pascher, W.; Den Besten, J. H.; Caprioli, D.; Lejtens, X.; Smit, M.; Van-Dijk, R.: Modelling and design of a travelling-wave electro-optic modulator on InP. Opt. Quantum Elec. **35** (2003), 453–464.
[25] Pregla, R.: Modeling of planar waveguides with anisotropic layers of variable thickness by the method of lines. Optical and Quantum Electronics **35** (2003), 533–544.
[26] Pregla, R.; Conradi, O.: Modeling of uniaxial anisotropic fibers with noncircular cross section by the method of lines. Journal of Lightwave Technology **21** (2003), 1294–1299.
[27] Conradi, O.; Helfert, S.; Pregla, R.: Modification of the finite difference scheme for efficient analysis of thin lossy metal layers in optical devices. Optical and Quantum Electronics **30** (1998), 369–373.
[28] Berini, P.: Plasmon-polariton waves guided by thin lossy metal films of finite width: Bound modes of symmetric structures. Phys. Rev. B **61** (2000), 10484–10503.
[29] Martin, O. J. F.; Piller, N. B.: Electromagnetic scattering in polarizable backgrounds. Phys. Rev. E **58** (1998), 3909–3915.
[30] Kottmann, J. P.; Martin, O. J. F.: Accurate solution of the volume integral equation for high permittivity scatterers. IEEE Trans. Antennas Propag. **48** (November 2000), 1719–1726.
[31] Paulus, M.; Gay-Balmaz, P.; Martin, O. J. F.: Accurate and efficient computation of the green's tensor for stratified media. Phys. Rev. E **62** (October 2000), 5797–5807.
[32] Paulus, M.; Martin, O. J. F.: A fully vectorial technique for scattering and propagation in three-dimensional stratified photonic structures. Opt. Quant. Electron. **33** (2001), 315–325.
[33] Paulus, M.; Martin, O. J. F.: Light propagation and scattering in stratified media: A green's tensor approach. J. Opt. Soc. Am. A **18** (April 2001), 854–861.
[34] Gay-Balmaz, P.; Martin, O. J. F.: Electromagnetic scattering of high permittivity particles on a substrate. Appl. Opt. **40** (2001), 4562–4568.
[35] Morse, P. M.; Feshbach, H.: Methods of theoretical physics. New York: McGraw-Hill, 1953.
[36] Paulus, M.; Martin, O. J. F.: How to tap an innocent waveguide. Opt. Express **8** (June 2001), 644–648.
[37] Yaghjian, A. D.: Electric dyadic green's functions in the source region. Proc. IEEE **68** (1980), 248–263.
[38] Morton, K. W.: Basic course in finite element methods. Comput. Phys. Rep. **6** (1987), 1–72.
[39] Cowper, G. R.: Gaussian quadrature formulas for triangles. Int. J. Numer. Methods Eng. **7** (1973), 405–408.
[40] Keast, P.: Moderate-degree tetrahedral quadrature formulas. Comp. Methods Appl. Mech. Eng. **55** (1986), 339–348.
[41] Girard, C.; Martin, O. J. F.; Dereux, A.: Molecular lifetime changes induced by nanometer scale optical fields. Phys. Rev. Lett. **17** (1995), 3098–3101.
[42] Martin, O. J. F.; Girard, C.; Dereux, A.: Generalized field propagator for electromagnetic scattering and light confinement. Phys. Rev. Lett. **74** (1995), 526–529.
[43] Martin, O. J. F.; Girard, C.; Smith, D. R.; Schultz, S.: Generalized field propagator for arbitrary finite size photonic bandgap structures. Phys. Rev. Lett. **82** (1999), 315–318.
[44] Flatau, P. J.: Improvements in the discrete-dipole approximation method of computing scattering and absorption. Opt. Lett. **22** (August 1997), 1205–1207.
[45] Nebeker, B. M.; Starr, G. W.; Hirleman, E. D.: Evaluation of iteration methods used when modeling scattering from features on surfaces using the discrete-dipole approximation. J. Quant. Spectrosc. Radiat. Transfer **60** (1998), 493–500.
[46] Cátedra, M. F.; Torres, R. P.; Basterrechea, J.; Gago, E.: The cg-fft method. Boston: Artech House, 1995.
[47] Schmehl, R.; Nebeker, B. M.; Hirleman, E. D.: Discrete-dipole approximation for scattering by features on surfaces by means of a two-dimensional fast fourier transform technique. J. Opt. Soc. Am. A **14** (November 1997), 3026–3036.
[48] Paulus, M.; Martin, O. J. F.: Scattering experiments with a diving cylinder. Opt. Express **9** (September 2001), 303–311.
[49] Barlatey, L.; Mosig, J. R.; Sphicopoulos, T.: Analysis of stacked microstrip patches with mixed potential integral equation. IEEE Trans. Antennas Propag. **38** (1990), 608–615.
[50] Mosig, J. R.; Alvarez-Melcon, A.: Green's tensor functions in layered media: imaginary axis integration and asymptotic behavior. IEEE Antennas and Propag. Soc. Int. Symposium, New York, 1996. IEEE, 416–19.
[51] Gay-Balmaz, P.; Mosig, J. R.: Three-dimensional planar radiating structures in stratified media. Int. J. Microwave and Millimeter wave CAE **3** (1997), 330–343.

Olivier J.F. Martin received the B.Sc. and Ph.D. degrees in physics in 1989 and 1994, respectively, from the Swiss Federal Institute of Technology, Lausanne (EPFL), Switzerland. In 1989, he joined IBM Zurich Research Laboratory, where he investigated thermal and optical properties of semiconductor laser diodes. Between 1994 and 1997 he was a research staff member at the Swiss Federal Institute of Technology, Zurich (ETHZ). In 1997 he received a Lecturer fellowship from the Swiss National Science Foundation (SNSF). During the period 1996–1999, he spent a year and a half in the U.S.A., as invited scientist at the University of California in San Diego. In 2001 he received a Professorship grant from the SNSF and became Professor of Nano-Optics at ETHZ. In 2003, he was appointed Professor of Nanophotonics and Optical Signal Processing at EPFL, where he is currently head of the Nanophotonics and Metrology Laboratory.
His research interests focus on the interactions of electromagnetic fields with low dimension systems, over a broad range of the spectrum and include activities both in optics and microwave regimes.
Dr. Martin has authored or co-authored over 130 scientific publications and a handful of patents and inventions disclosures.